Computers and Concrete, *Vol. 24, No. 3* (*2019*) *271-282*
DOI: https://doi.org/10.12989/cac.2019.24.3.271

Leveraging artificial intelligence to assess explosive spalling in fire-exposed RC columns

A. Seitllari[1] and M.Z. Naser*[2]

[1]*Department of Civil and Environmental Engineering, Michigan State University, MI, USA*
[2]*Glenn Department of Civil Engineering, Clemson University, SC, USA*

(*Received February 26, 2019, Revised July 23, 2019, Accepted August 6, 2019*)

Abstract. Concrete undergoes a series of thermo-based physio-chemical changes once exposed to elevated temperatures. Such changes adversely alter the composition of concrete and oftentimes lead to fire-induced explosive spalling. Spalling is a multi-dimensional, complex and most of all sophisticated phenomenon with the potential to cause significant damage to fire-exposed concrete structures. Despite past and recent research efforts, we continue to be short of a systematic methodology that is able of accurately assessing the tendency of concrete to spall under fire conditions. In order to bridge this knowledge gap, this study explores integrating novel artificial intelligence (AI) techniques; namely, artificial neural network (ANN), adaptive neuro-fuzzy inference system (ANFIS) and genetic algorithm (GA), together with traditional statistical analysis (multilinear regression (MLR)), to arrive at state-of-the-art procedures to predict occurrence of fire-induced spalling. Through a comprehensive data-driven examination of actual fire tests, this study demonstrates that AI techniques provide attractive tools capable of predicting fire-induced spalling phenomenon with high precision.

Keywords: concrete; fire; spalling; artificial intelligence

1. Introduction

Fire is a destructive force in nature. Unlike other loading conditions, i.e., wind, earthquake, blast etc., fire can damage structures on two fronts. In the first, high temperatures can trigger micro-structure transformation within construction materials, leading to material softening and weakening (Khoury 2000). In the second front, fire effects may also alter geometrical features of structures (or structural members for the matter). In this scenario, the adverse effects of fire, either directly (i.e., through flames and combustion) or indirectly (e.g., fire-induced phenomenon etc.), can damage structural integrity and/or load bearing capabilities via reduction in member's effective cross section (as in charring of wood members, buckling of steel members or spalling in concrete members) (Naser 2011). The latter is the focal point of this work.

Concrete is an inert material and a poor heat conductor which makes it attractive for fire engineering applications (Erdem 2017, Ibrahimbegovic *et al.* 2010, Naser and Chehab 2018). As a result, concrete structures rarely require external fire proofing. In fact, building codes and standards lists standardized fire resistance ratings for various concrete-based structural members (BSI and European Committee for Standardization 2004). These ratings often associate a given fire resistance time (i.e., duration of 2 hours to fire exposure) with member's cross-sectional dimensions (e.g., width or depth and/or concrete cover to interior steel reinforcement). Hence, fire designers may simply pick a suitable memberal configuration to satisfy fire codal provisions. While this practice has been well-documented and proven effective, this has also been shown to underestimate available fire resistance in concrete structural members and been criticized as a result of numerous fire incidents and their post-fire investigations (Meacham *et al.* 2009, Peris-Sayol *et al.* 2017).

It is worth noting that such criticism primarily stems from the fact that standardized fire ratings were developed as a result of comprehensive testing programs carried out few decades ago. Such tests were conducted on concrete materials available in the 1960-70s which, quite frankly, share little resemblance to modern concretes given the tremendous advancement in material sciences nowadays. Traditional concretes are made of a mixture of sand, cement, aggregates, and water. Thus, these concretes have simple micro-structure, relatively high porosity and are hence often referred to as traditional concretes (i.e., normal strength concrete (NSC)). On the other hand, modern concretes comprise of above components, together with advanced admixtures, fillers, and additives, all of which complicate mixture homogeneity as well as alter key chemical and physical characteristics of concrete (Phan and Carino 2000). Some of the modern types of concrete include high strength concrete (HSC), high performance concrete (HPC), fiber reinforced concrete (FRC) etc. A key point to remember is that modern concretes are essentially designed to outperform and replace traditional concretes and hence are specifically tailored to have high strength (dense micro-structure) and durability features (i.e., low permeability to mitigate corrosion of steel reinforcement)

*Corresponding author, Assistant Professor
E-mail: mznaser@clemson.edu

http://www.techno-press.org/?journal=cac&subpage=8 ISSN: 1598-8198 (Print), 1598-818X (Online)

(Kodur 2018).

While such properties are ideal for ambient working conditions (viz. high-rise buildings/marine and transportation infrastructures), the same properties are unfavored once concrete is exposed to elevated temperatures. This is due to the fact that the dense nature of modern concretes, when combined with its low permeability, tend to trap water moisture within concrete for prolong periods of time. Under fire conditions, generated heat evaporates this moisture which then turns into water vapor. Vapor accumulates within capillary voids/pores and once vapor pressure exceeds a threshold (i.e., tensile strength of concrete), concrete spalls (Klingsch 2014). This phenomenon occurs under fire conditions, and as such measures to mitigate fire-induced spalling are seldom put into place due to the fact the building codes continue to recognize fire as a primary loading effect. As such, fire rarely governs the design of a structure as opposed to other loading effects such as wind or earthquake loading etc. (CEN 2002).

A number of researchers examined fire-induced spalling phenomenon through classical means i.e., experimentations (Boström *et al.* 2018, Kalifa *et al.* 2001, Zhang *et al.* 2016), numerical simulations (Dwaikat and Kodur 2009), analytical works (Bažant and Thonguthai 1979) etc. A close look into these works shows that they tend to involve a tedious procedure and been only verified against few tests. Hence, the applicability of traditional methods to evaluate concrete's tendency to spall under fire conditions might not be viable nor easily applied. In order to overcome some of the challenges and limitations associated with previously developed methodologies, this study explores the potential of utilizing artificial intelligence (AI) into comprehending the process of fire-induced spalling in concrete structures. In recent years, AI has become an attractive and promising technique to solve complex and seemingly random engineering phenomena (Boussabaine 1996, Cobaner, *et al.* 2009, Kisi and Çobaner 2009, Lee *et al.* 2004, Seitllari *et al.* 2019, Naser *et al.* 2012, Naser 2018, Seitllari 2014, Seitllari and Kutay 2018). A major advantage of AI is its capability to learn from observations and patterns and ability to produce predictive models; potentially waving the necessity for expensive and cumbersome experimental works. In the context of concrete materials and structures, AI has been employed in a multitude of perspectives as documented in recent studies (Ashteyat and Ismeik 2018, Asteris and Kolovos 2017, Bilgehan and Kurtoğlu 2016, Eredm *et al.* 2013, Hodhod *et al.* 2018, Lingam and Karthikeyan 2014, Mansouri *et al.* 2018, Mansouri and Kisi 2015, Naser *et al.* 2012, Naser and Seitllari 2019, Saha and Kumar 2017, Yavuz 2019).

In this work, the application of traditional analysis (viz. multilinear regression (MLR)), and AI computing techniques namely: artificial neural network (ANN), adaptive neuro-fuzzy interface system (ANFIS), and genetic algorithm (GA), are implemented to develop predictive models for fire-induced spalling in concrete structural members. The proposed models take into account geometric (cross sectional dimensions and thickness of concrete cover), material (concrete type and compressive strength) as well as loading features (i.e., concentric or eccentric loading) when evaluating fire-induced spalling of reinforced concrete (RC) columns. Furthermore, these models implicitly account for high temperature material properties of constituent materials, and as such do not require input of such properties nor special solution framework. The validity of these models was examined against actual fire-tested RC columns collected from various fire tests.

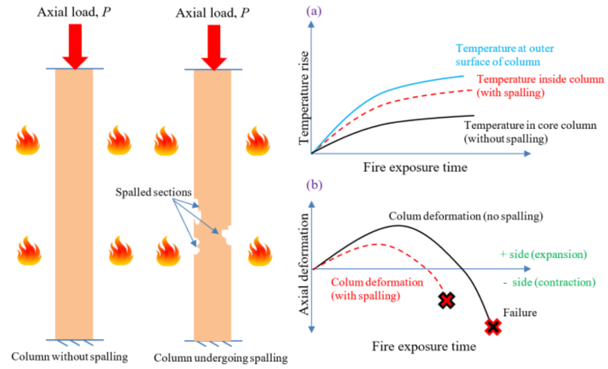

Fig. 1 Typical response of RC columns under fire conditions

2. Fire-Induced explosive spalling in concrete columns – An overview

Before introducing the developed AI methodology, a concise review on fire behavior of RC columns is beneficial to understand the complexity of fire-induced explosive spalling in such members. When fire breaks out, cross-sectional temperature in surrounding structural members (say a RC column) starts to slowly rise. This slow rise in temperature is due to the inherently low thermal conductivity and high specific heat of concrete as well as presence of moisture (in concrete micro-structure). As a result, a significant amount of heat is required to raise temperature in concrete. Thus, in the initial stage of fire, a thermal gradient develops in which the temperature at the exposed surface of concrete is much higher than that at the inner layers of concrete[1] (see Fig. 1(a)). At this stage, the fire-exposed RC column typically expands, under higher load it will only contract as shown in Fig. 1(b). Later on, and due to the rise in cross-sectional temperature and associated degradation in strength properties, the column starts to weaken. This corresponds to a contraction stage in which the axial deformation of the column decreases and shifts from an expansion-controlled (noted in the positive side of Fig. 1(b) into a contraction-controlled (noted in the negative side of the same figure).

With the continuous rise in sectional temperature, the strength and Young's modulus properties of both concrete

[1] While steel reinforcement has much higher thermal conductivity and lower specific heat than concrete, the temperature in steel can still be assumed to be similar to that of the surrounding concrete (as the area of reinforcement is very small as compared to that of concrete cross-section).

and steel reinforcement starts to degrade. This degradation is slow as it reflects the reliance on concrete material under elevated temperatures. Still, the degradation in strength and Young's modulus properties could be accelerated by fire-induced effects such as spalling of concrete. Spalling can be broadly grouped under two classes; explosive spalling and corner spalling (Khoury 2000). Explosive spalling tends to occur violently and during the early stages of fire exposure and this type of spalling is primarily governed by the development of pore pressure facilitated by moisture migration as well as the development of thermal gradients; once temperature in concrete layers reaches 220-280°C (Liu *et al.* 2018). On the other hand, corner spalling mainly occurs gradually and along the edges of members due to unrestrained thermal expansion in the transverse direction. In either case, once spalling occurs, a reduction in cross-sectional mass of concrete column is expected and with the increase of fire exposure duration and further losses in mechanical properties of concrete and reinforcing steel, the column eventually fails. In general, a RC column undergoing spalling is prone to fail before a similar column that does not undergo spalling (given that both are subjected to similar loading and fire conditions).

3. Data collection

In order to feed the developed AI-based models, a literature review was first carried out to collect studies and data points from fire tests associated with fire-induced spalling. In this process, notable works were identified and then reviewed (Hass 1986, Kodurand McGrath 2003, Kodur *et al.* 2001, Kodur *et al.* 2000, Lie and Woollerton 1988, Myllymaki and Lie 1991, Rodrigues *et al.* 2010). From these studies, critical factors were extracted including geometrical, material, loading and spalling features of fire-tested RC columns. For example, the National Research Council of Canada (NRCC) carried out a number of research programs to examine the behavior of RC columns made of normal strength, high strength, and high-performance concretes under fire. In one study, Lie and Woollerton (Lie and Woollerton 1988) tested 41 RC columns under standard fire conditions while varying shape (square, rectangular, and circular), cross-sectional size (203×203 mm^2–406×406 mm^2), ratio of longitudinal steel rebars (2.19–3.97%), type of aggregate (carbonate, siliceous and lightweight), compressive strength of concrete (34-42 MPa), load magnitude (0–90%).

In a separate testing program, Kodur *et al*. (Kodurand McGrath 2003, Kodur *et al*. 2001, 2000) carried out fire tests on high strength and high-performance RC columns and noted the tendency of these columns to fire-induced spalling. In their tests, Kodur *et al*. (Kodurand McGrat, 2003, Kodur *et al*. 2001, 2000) varied a number of features such as spacing of ties, as well as loading configuration (i.e., eccentricity). More recently, Shah and Sharma (Shah and Sharma 2017) conducted fire resistance experiments on 8 RC columns, 6 that were made of normal strength concrete and 2 comprising of high strength concrete. These 8 columns were longitudinally reinforced with eight steel rebars each of 16 mm diameter and were embedded behind 40 mm concrete cover. Other fire tests were also carried out by Myllymi and Lie (1991), Rodrigues *et al*. (2010). It should be noted that a complete list of the 89 selected columns is provided in Table A in the Appendix.

4. Methodology and rationale

This section summarizes both mathematical and computational aspects of the traditional analysis procedure and AI computing techniques. Four techniques, namely: multilinear regression (MLR), adaptive neuro-fuzzy interface system (ANFIS), artificial neural network (ANN) and genetic algorithm (GA) were used to develop predictive models for fire-induced spalling in concrete. Detailed descriptions of these modeling approaches are provided herein.

4.1 Multi-Linear Regression (MLR)

The multi-linear regression method attempts to establish a relation between two (or more independent variables) and one dependent variable by means of fitting a linear equation into experimental (measured) data points. For example, consider y to be the response (dependent variable), and a_1, a_2..., a_z to be predictor variables, thus the MLR equation can be defined using Eq. (1)

$$y = \xi_0 + \xi_1 a_1 + \xi_2 a_2 + \ldots + \xi_z a_z \tag{1}$$

where ξ_0 is the intercept regression coefficient, ξ_1, ξ_2..., ξ_z are the regression parameters projected using the least-square error between the estimated and experimental response (Chapra and Raymond 2010).

Before the MLR model is developed, the input arguments are selected based on the principal analysis concept (Bro and Smilde 2014). The main idea of this concept is to investigate the influence of each input variable on the response (dependent variable) and then only select the most influential input variables for further consideration. Thus, the available experimental data points were randomly separated into two groups including a training set and a testing set. The training set (≈80% of the data points) comprised of the model regression coefficient determination of MLR. The predictive strength of the MLR generated model was then validated using the testing set (≈20% of the data points). According to the resultant sensitivity analysis, a potential correlation was distinguished among the following input combinations: compressive strength of concrete (f_c), the width of RC column (*Brc*), the magnitude of loading eccentricity (*e*), and magnitude of applied loading (*P*). As such these parameters were chosen to be input variables.

4.2 Artificial Neural Networks (ANNs)

The conceptual design of an artificial neural network (ANN) mimics the biological neural network of the brain. This technique is known for its ability to break down and solve very complex and/or nonlinear problems using simple mathematical operations (Kisi and Çobaner 2009). In ANN, artificial neurons act as processing hubs and use mathematical functions to determine the behavior of received inputs/data points. This study applied a commonly used type of ANNs known as multi-layer feed-forward neural network. This ANN is structured by interconnected neurons, grouped in layers with each layer fully connected to the successive layer (see Fig. 2). It is worth noting that recent studies have reported that ANN can be a promising technique for understanding the nature of complex phenomena and hence is its potential is examined herein (Boussabaine 1996, Lee *et al*. 2004, Naji *et al*. 2016, Naser *et al*. 2012, Seitllari 2014, Seitllari and Kutay 2018)

Once input into the first layer, input data flows only from the input layer towards hidden and output layers. Every neuron processes the received input vector and relays the information to the following layer through specific connections. The process of forward flowing of data is known as the feed-forward network. The model development consists of two main processing phases: training and testing. For a given set of data, the training phase of multi-layer feed-forward neural network befits in arranging various weights to acceptable limits. This process continues for a pre-defined number of iterations and/or as long as a pre-specified error tolerance is achieved between experimental and ANN-predicted output. After the training process is finalized, it is expected that the retrieved results to be very similar to the data provided for the training phase. Usually, the network training process is performed using back-propagation algorithm by minimizing the error between the input and output layers and adjust the weights in reverse direction after each iteration cycle (Kisi and Çobaner 2009). The most commonly used optimization method is Leveberg-Marquard which, evaluates the error in terms of Mean Squared Error (MSE). In this method, if z is the experimental dataset, then MSE can be calculated using Eq. (2).

$$MSE = \frac{1}{z}\sum_{i=0}^{z}(e_i)^2 = \frac{1}{z}\sum_{i=0}^{z}(m_i - p_i)^2 \tag{2}$$

where, z=the total number of datasets, e_i=the error for each input set, m_i=the measured output, and p_i=the estimated output.

There are three steps used for determining an optimal ANN topology and these steps include: (i) determining the preliminary structure, (ii) training the network and (iii) testing the network. The ANN can be characterized by a number of layers wherein each layer serves as a set of parallel nodes. In this study, a three-layer ANN structure, with only one intermediate layer, is used (see Fig. 2). By using neurons in the hidden layer, the network can learn and recognize the relevant data patterns and approximate complex nonlinear mapping (transformation) between the input and output datasets.

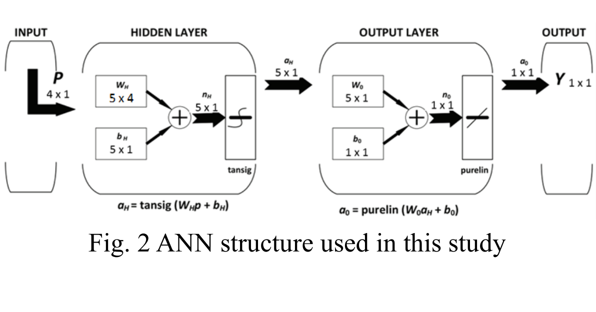

Fig. 2 ANN structure used in this study

The activated transfer function processes the data and then the hidden layer passes the results (i.e., final values) to the output layer. The abbreviations are shown in Fig. 2, W_H and W_O, represent the interconnection weights for the hidden layer and output layer, respectively. Likewise, b_H and b_O are the biases for hidden layer and output layers, respectively. The ANN developed herein employed a trial and error procedure to determine the best network design/topology. Logistic (a.k.atansig: a_H=2/(1+exp(-2*p))-1)) and linear (a_O=purelin (a_H)) transfer functions were observed to perform more accurately for hidden layer and output layer, respectively (Cobaner *et al*. 2009). The best-fitting model was statistically evaluated in terms of MSE as well as coefficient of determination (R^2) and mean absolute relative error (MARE) (see Eqs. (3)-(4) below). The predictive capability of the ANN model was evaluated on the same training and testing data sets used for MLR model development.

$$\mathrm{R}^2 = \frac{\Sigma(m_i - p_i)^2}{\Sigma(p_i - p_{avg})^2} \tag{3}$$

$$\mathrm{MARE} = \frac{1}{z}\sum_{i=1}^{z}\left|\frac{m_i - p_i}{m_i}\right| \times 100 \tag{4}$$

where, p_{avg}=the average estimate output.

4.3 Adaptive Neuro-Fuzzy Interface System (ANFIS)

Adaptive Neuro-Fuzzy Interface System (ANFIS) is a multilayer adaptive network-based fuzzy inference system that was introduced by Jang *et al.* (1997). This technique is known for its capability to implement hybrid learning procedure thus, enabling neural network to mimic the linguistic approach of expert knowledge systems (i.e., if-then rules) without precise quantitative analysis. The structure of this fuzzy inference system consists of a number of nodes which are connected through directional links. Each node is identified by a function with a fixed or adjustable parameter. The learning stage of fuzzy systems uses error minimization techniques to match the parameter values with the pre-determined training data set. The most common learning algorithm is the back-propagation learning algorithm which allows the fuzzy system to adjust the relations between layers by minimizing the sum of squared differences using the training data set (Daldaban, *et al*. 2006).

Besides numerical variables, the fuzzy method also applies verbal/logical labels. The "if-then" rules (or fuzzy conditional statements) are employed to capture the imprecise cognizance between the fuzzy variables. The initial concept and basic principles of fuzzy systems were first introduced by Zadeh (1995) as to be applied in scenarios where vague linguistic statements are often used to drive uncertainties in different control mechanism. According to Zadeh (1995), while experts thinking cannot be correlated to certain (quantitative) values, this can still be conveyed through levels of fuzzy sets. This procedure utilizes an "if-then" rule system. For example, this process

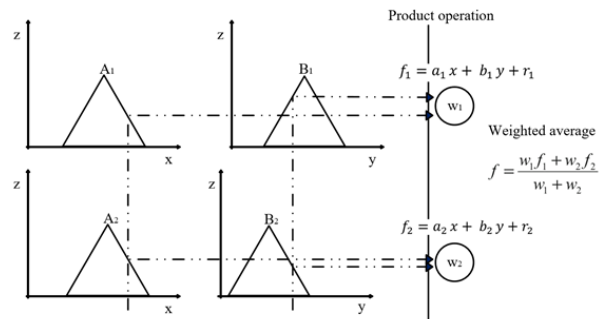

Fig. 3 The first order Tagaki-Sugeno fuzzy model with two rules and two inputs

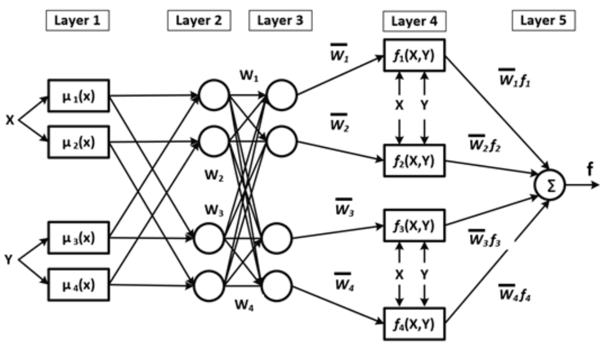

Fig. 4 Equivalent ANFIS architecture

involves mapping of a certain set to a fuzzy set interval. This so called mapping is enabled through the membership functions which are used to numerically define the partial belonging of a statement by assigning values between 0 and 1. Thus, in the case of uncertainty, the variable is known to be fuzzy and is approximated on a compact set through a membership function. Typically, the membership function is imparted in linear form for computational simplicity (Zadeh 1995). It is noteworthy that the fuzzy inference system alone has significant adaptation difficulties with changing external environment. However, the association of neural networks with the fuzzy inference system was intended to overcome this issue by introducing the new concept called adaptive neuro-fuzzy inference approach.

This study applied the first order Tagaki-Sugeno model due to its compactness and computational efficiency (Cobaner 2011). This fuzzy reasoning system comprises of two inputs x and y. The first order Tagaki-Sugeno fuzzy model is set with two "if-then" rules, as can be shown by the following formulations

$$Rule\ 1: If\ x\ is\ A_1\ and\ y\ is\ B_1, then\ f_1 = a_1 x + b_1 y + r_1 \tag{5}$$

$$Rule\ 2: If\ x\ is\ A_2\ and\ y\ is\ B_2, then\ f_2 = a_2 x + b_2 y + r_2 \tag{6}$$

where x, y = input arguments, A, B = the linguistic labels, a, b, r=output function parameters.

The schematic demonstration of this approach is visually illustrated in Fig. 3. The resulting output is the so-called crisp value which is the weighted average of each output rule.

An illustrative example of a typical fuzzy inference system prototype for two inputs (x and y) is illustrated in Fig. 4. As illustrated in Fig. 4, a fuzzy inference system contains five layers mainly; fuzzification layer (Layer 1), rule inference layer (Layer 2), normalization layer (Layer 3), defuzzification layer (Layer 4) and the final output layer (Layer 5) briefly explained as follows:

Layer 1: every node i in this layer is an adaptive node characterized by bell function, e.g.

$$\mu_i(x) = \frac{1}{1 + |\frac{x - \delta_1}{\alpha_1}|^{2\beta_1}} \tag{7}$$

where $\mu_i(x)$=i^{th} resultant of 1st layer, x=node input, α_1, β_1, δ_1=parameter set. Parameters of the first layer are usually denoted as the premise set. The resultants of the first layer are the membership values of the premise part.

Layer 2: this layer comprises nodes that multiply incoming signals and send the product of this multiplication to the next layer. The output of each node indicates thefiring strength of a given rule.

$$W_i = \mu_{ki}(x)\mu_{li}(y), \mathrm{i} = 1, 2, \ldots \tag{8}$$

where W_i =2nd layer i^{th} output, $\mu_{ki}(x)$, $\mu_{li}(y)$ = signals coming from the 1st layer.

Layer 3: this layer encompasses nodes which compute the ratio of the i^{th} rule's firing strength to the summed value of all rules' firing strengths. The resultant of this layer is known as the normalized firing strength

$$\bar{W}_{\mathrm{i}} = \frac{W_{\mathrm{i}}}{W_1 + W_2 + W_3 + W_4}, \mathrm{i} = 1, 2, \ldots \tag{9}$$

Layer 4: this layer's nodes are adaptive with node functions.

$$\bar{W}_i f_i = \bar{W}_i(a_i x + b_i y + r_i), \mathrm{i} = 1, 2, \ldots \tag{10}$$

where $\bar{W}_i$=3rd layer i^{th} output, $a_i, b_{i,} c_i$ =parameter set.

Layer 5: this layer's single node computes the final output as described in Eq. (11) the summation of all incoming signals.

$$f = \sum_{i=1}^{n} W_i f_i \tag{11}$$

Further description of ANFIS can be found in Jang (Jang *et al*. 1997).

Various ANFIS structures for the selected input parameters (i.e., Brc, f_c, e, P) were input into the program code including fuzzy toolbox developed in MATLAB. The generated ANFIS structures; especially the topology that gave the highest R^2 and minimum MSE and MARE were selected. Two Gaussian membership functions to the NF models were found enough for modeling fire-induced spalling. The necessary details of the selected model are also provided in the next section.

4.4 Genetic Algorithm (GA)

Genetic algorithm is an evolutionary technique that was introduced by Koza (1992) and utilizes supervised programs to solve a given phenomenon through principles

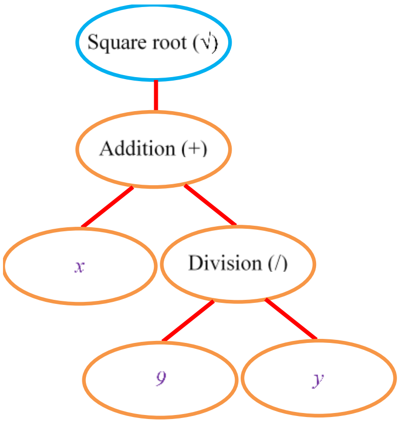

Fig. 5 Typical tree representation for √(x+(9/y)) in GA

of Darwinian selection. In this soft computing technique, predefined algorithms search a program space instead of a data space to arrive at mathematical representations. In GA, a random population of individuals often referred to as "trees" is created to house a number of possible solutions through the structural ordering of mathematical symbols. Thus, a possible solution in GA is a ranked tree consisting of functions and terminals. For example, a function (F) may contains basic mathematical operations (addition "+", multiplication "×" etc.), power functions (logarithm "log", exponential "exp"), conditional functions (Greater than ">", less than "<" etc.), Logic functions ("AND", "OR", "NOR", "NAND" etc.), among others. On the other hand, the terminal (T) comprises of arguments as well as numerical constants and/or variables, etc. Both functions and terminals are first randomly generated and then joined together to make a model. Hence, a developed model has a tree-like formation (configuration) in which branches can extend from a function and end in a terminal as shown in Fig. 5.

Once a set of models is arrived at, the GA evaluates the fitness (accuracy) of each model for reproduction. The fitness of a model is defined as a value that best reflects how good the model's predicted results are from that observed in experiments. The fittest models are then selected and manipulated by a number of operations i.e., reproduction, crossover and mutation (Koza 1992). While the reproduction operation gives a higher probability of selection to more successful models, the crossover operation ensures the exchange of genetic material between the evolved models. In the mutation operation, the GA randomly selects a function (or terminal) from a model to mutate. For example, if a mutation is carried out on a tree, then a new function node is chosen and the original node together with its relative sub-tree is replaced by a new randomly created sub-tree. Finally, the fitness for all of the processed models is calculated and is terminated once a convergence condition is met.

5. Results and discussion

In the current study, concrete strength (f_c), width of RC column (Brc), magnitude of eccentricity (e) and loading (P) were used as input parameters to multi-linear regression (MLR), artificial neural network (ANN), adaptive neuro-fuzzy system (ANFIS) and genetic algorithm (GA) to evaluate occurrence of fire-induced explosive spalling in RC columns. In order to assess the capability of the applied techniques, the testing and training data sets were fixed hence; each technique was fed with the same input data set values. The data set selection process for both the training set and testing set was statistically evaluated as presented in Table 1.

Table 1 Data statistics for training and testing

Input	$\bar{X}$*	s_x	c_{sx}	x_{min}	x_{max}
	Training Phase				
Concrete strength, f_c	59.4	31.0	1.09	24	138
RC column width, Brc (mm)	316.4	47.3	0.71	203	406
Magnitude of eccentricity, e (mm)	36.8	38.4	2	0	40
Applied loading, P (kN)	1647	1187	1.41	0	4981
	Testing Phase				
Input	$\bar{X}$	s_x	c_{sx}	x_{min}	x_{max}
Concrete strength, f_c	66.2	38.3	0.73	28	138
RC column width, Brc (mm)	337.6	49.8	0.77	300	406
Magnitude of eccentricity, e (mm)	5.9	11.4	1.64	0	40
Applied loading, P (kN)	2152	1605	0.83	0	5373

* $\bar{X}$: overall mean; s_x: standard deviation; c_{sx}: skewness coefficient; x_{min}: minimum; x_{max}: maximum

It can be seen that the magnitude of eccentricity (e) shows the highest skewed distribution (2.0 for the training set and 1.64 for the testing set), followed by the load (P). This table also shows that the presented values confirm strong statistical correlations of the selected data points. The developed models' statistical evaluation was determined using mean-squared error (MSE), mean absolute relative error (MARE), and coefficient of determination (R^2). It is noteworthy that R^2 indicates the degree at which the predicted and measured values are linearly related. The higher R^2 is, the better the prediction for the developed model. Whereas, MSE and MARE values are more useful for providing information on the predictive performance of the developed model. In contrary to R^2, the smaller MSE and MARE, represent high precision and accuracy for a given model.

Table 2 shows the statistical criteria of different models developed based on the above-mentioned computing methods. The high value of R^2 indicates that there is a good correlation between the measured values and predicted values estimated by the computing methods in the training phase. This table shows that the GA performs with the highest precision with R^2=0.95 in the training phase and R^2=0.80 in the testing phase, thus outperforming the other methods and closely followed by ANN, ANFIS, and MLR. Similarly, the same ranking is observed for the other two statistical parameters, however, with ANN having the lowest MSE and MARE and as expected MLR having the highest MSE. Interestingly, GA's MARE value was observed to be the highest. According to the obtained results, it can be said that the ANN and GA methods demonstrate better simulation efficiency as compared to

Table 2 *MSE*, *MARE* and R^2 statistics the developed models

Method	Training Phase		
	MSE	*MARE*	R^2
MLR	29.57	0.17	0.30
ANN	16.77	0.10	0.61
ANFIS	25.71	0.15	0.39
GA	0.01	0.23	0.95
Method	Testing Phase		
	MSE	*MARE*	R^2
MLR	22.17	0.13	0.49
ANN	12.27	0.06	0.78
ANFIS	21.06	0.12	0.53
GA	0.06	0.89	0.80

developed ANFIS and MLR models. From the obtained statistics, it can be inferred that the MLR and ANFIS approaches did not yield accurate prediction. It was also clear that the proposed GA model could generalize better than the preceding two methods followed by ANN model which, demonstrated satisfying performance in estimating the complex phenomena of spalling occurrence in RC columns.

Fig. 6 illustrates the predicted spalling phenomenon by the four computing methods against the experimental results for the training dataset and testing dataset, respectively. The results were evaluated considering the model response as follows; *1-spalling occurred*, and *2-no*

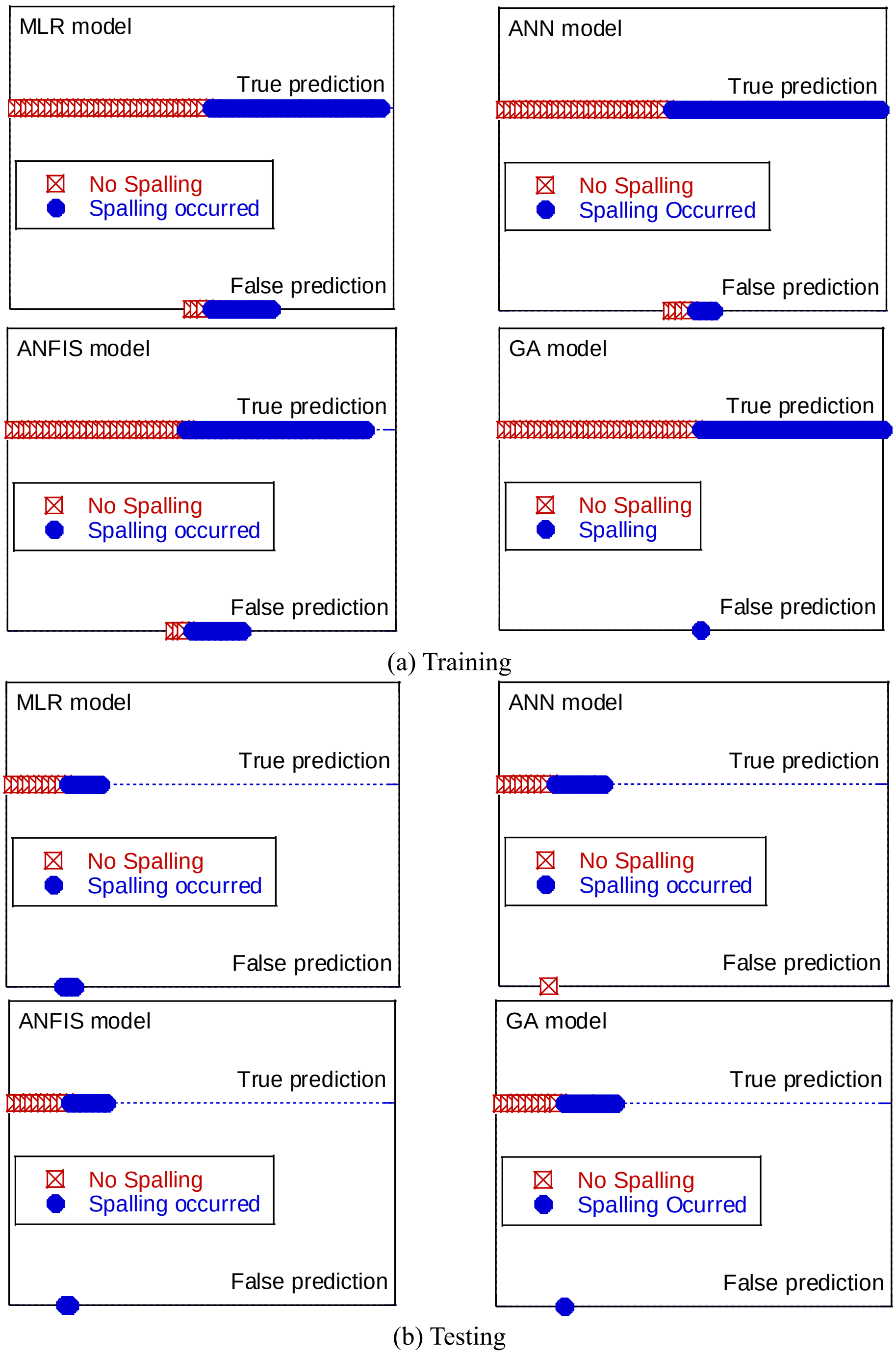

Fig. 6 Performance of applied AI techniques in (a) training and (b) testing

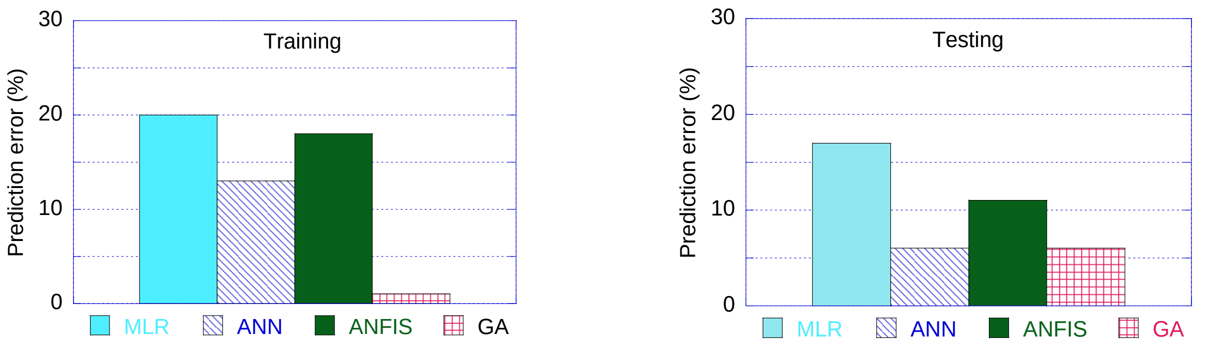

Fig. 7 The error performance of AI-based techniques

Table 3 The computed model expressions to be used for evaluating the spalling occurrence on RC columns

	Technique	Model details							
Fire-induced spalling	MLR	$Spalling = 2.213 - 11.39 \times 10^{-3} f_c - 71 \times 10^{-5} Brc - 10^{-7} e - 99 \times 10^{-6} P$							
	ANN[+]	Weight matrix for the hidden layer (W_H)					Bias vector for the hidden layer (b_H)	Weight vector of the output layer (W_0)	Bias for the output layer (b_0)
		Element/neuron no. in each layer	1	2	3	4			
		1	-2.84	4.9	-5.74	-1.04	-0.97	-1.55	-0.6
		2	-1.51	-11.1	1.04	0.23	5.65	-2.65	
		3	-0.28	-5.6	-4.12	-0.97	6.06	0.64	
		4	-5.23	1.2	3.76	-0.42	0.91	1.4	
		5	-1.53	-8.83	1.16	0.97	3.33	1.71	
	ANFIS	Epoch number	Number of membership functions		Membership functions type		Fuzzy type		
		5	2-2-2-2		Gaussian		Sugeno		
	GA[*]	$Spalling = Logistic\left(473.3 - \frac{248191.5\sin(Brc) - 112.76e\sin(-8.286e - 8.286P) - 112.8P\sin(-8.286e - 8.286P)}{146 - e - P} - 6.89 f_c - 97.3\sin\left(\frac{3.38e + 3.38P}{f_c}\right)\right)$							

[+] When the ANN tabulated data are used to feed the ANN structure, one must follow Figure 2 details
[*]GA: this model was developed to yield *0* for *Spalling*, and *1* for *No spalling* and the logistic function used is $\mathbf{1/(1+e^{-x})}$. This equation is also provided in a spreadsheet that is accompanying this work

spalling occurred[2]. It can be inferred from these figures that the prediction of spalling phenomena using GA and ANN methods are closer to the actual observations as compared to the other developed methods in both training phase and testing phase. Moreover, MLR and ANFIS have the largest difference between the observed and predicted occurrences.

Fig. 7 shows error prediction for each method observed in both the training phase and the testing phase. Overall, the results clearly support the applicability of GA and ANN to predict the complex nature of fire-induced spalling in RC columns with high precision. This can be attributed to the nature of these techniques in which they can better comprehend complex phenomenon than that of traditional MLR. Surprisingly, predictions obtained from ANFIS are much poorer than that from ANN and GA, even though this technique acts in a similar form to ANN. This could be related to the different nature of this computing technique and the limited number of input data points (i.e., 89 fire tests) used to analyze this phenomenon.

In practice, engineers can apply the models presented in this research and listed in Table 3 (as well as companion works (Naser 2019, Naser and Seitllari 2019)) to evaluate the tendency of concrete columns to spall under fire. These models comprehend the vulnerability of RC columns to fire-induced spalling and may provide an easy tool to researchers and engineers given that there is a serious lack of methods/approaches that can be used to predict the occurrence of fire-induced spalling. In fact, current fire codes and standards still do not provide any assessment methods/approaches to evaluate fire-induced spalling in concrete. The developed expressions can serve as a benchmark (i.e., first generation) to realize such methods/approaches. We are confident that the methodology carried out herein can be utilized to refine the developed models upon the availability of new datasets measured in fire tests. While this section delivered a picture of statistically influencing factors that govern the occurrence of fire-induced spalling in concrete structures, it is worth noting that a more comprehensive review on other influencing parameters such as mix proportion (e.g., cement type, degree of moisture content, fibers, admixtures, etc.), grade, size and type (FRP vs. steel) of internal reinforcement, restraint conditions, maximum temperature reached, cooling phase, etc.) should also be used to investigate spalling behavior of concrete structures.

[2]Except in the case of GA, where this model was developed to yield 0 for No spalling, and 1 for Spalling

6. Conclusions

This study explores the merit of utilizing various artificial intelligence (AI) techniques to develop high precision procedures (models) with the ability to predict the occurrence of fire-induced explosive spalling in RC columns. These models are easy-to-implement and implicitly account for temperature-dependent material degradation. Other conclusions, as obtained from this work, are listed herein:

- Integrating AI-based methodologies seems to be effective in evaluating the response of structural members under fire conditions. These methodologies are particularly useful to identify the vulnerability of RC columns to fire-induced spalling.
- Both genetic algorithms and neural networks capture the tendency of RC columns to spall under fire conditions with high precision; outperforming ANFIS and MLR techniques.
- A proper AI analysis requires the availability of wealth of data points and/or observations obtained from fire tests. To this day, few works reported the outcome of fire tests, with special consideration to fire-induced spalling or examining various geometric, material and loading features that may directly affect the occurrence of spalling.

References

Ashteyat, A.M. and Ismeik, M. (2018), "Predicting residual compressive strength of self-compacted concrete under various temperatures and relative humidity conditions by artificial neural networks", *Comput. Concrete*, **21**(1), 47. https://doi.org/10.12989/CAC.2018.21.1.047.

Asteris, P.G. and Kolovos, K.G. (2017), "Self-compacting concrete strength prediction using surrogate models", *Neur. Comput. Appl.*, **31**(1), 1-16. https://doi.org/10.1007/s00521-017-3007-7.

Bažant, Z.P. and Thonguthai, W. (1979), "Pore pressure in heated concrete walls: theoretical prediction", *Mag. Concrete Res.*, **31**(107), 67-76. https://doi.org/10.1680/macr.1979.31.107.67.

Bilgehan, M. and Kurtoğlu, A.E. (2016), "ANFIS-based prediction of moment capacity of reinforced concrete slabs exposed to fire", *Neur. Comput. Appl.*, **27**(4), 869-881. https://doi.org/10.1007/s00521-015-1902-3.

Boström, L., McNamee, R., Albrektsson, J. and Johansson, P. (2018), "Screening test methods for determination of fire spalling of concrete", RISE Report.

Boussabaine, A.H. (1996), "The use of artificial neural networks in construction management: a review", *Constr. Manage. Econom.*, **14**(5), 427-436. https://doi.org/10.1080/014461996373296.

Bro, R. and Smilde, A. (2014), "Principal component analysis", *Anal. Meth.*, **6**(9), 2812. https://doi.org/10.1039/c3ay41907j.

BSI, and European Committee for Standardization (2004), Design of Concrete Structures -Part 1-2: General Rules -Structural Fire Design, Eurocode2 §. https://doi.org/10.1002/jcp.25002.

Buch, S.H. and Sharma, U.K. (2019), "Fire resistance of eccentrically loaded reinforced concrete columns", *Fire Technol.*, 1-36. https://doi.org/10.1007/s10694-019-00823-x

CEN (2002), Eurocode 1: Actions on Structures-Part 1-2: General Actions-Actions on Structures Exposed to Fire.

Chapra, S.C. and Raymond, C.P. (2010), *Numerical Methods for Engineers*, 6th Edition, McGraw-Hill,New York.

Cobaner, M. (2011), "Evapotranspiration estimation by two different neuro-fuzzy inference systems", *J. Hydrol.*, **398**(3-4), 292-302. https://doi.org/10.1016/J.JHYDROL.2010.12.030.

Cobaner, M., Unal, B. and Kisi, O. (2009), "Suspended sediment concentration estimation by an adaptive neuro-fuzzy and neural network approaches using hydro-meteorological data", *J. Hydrol.*, **367**(1-2), 52-61. https://doi.org/10.1016/J.JHYDROL.2008.12.024.

Daldaban, F., Ustkoyuncu, N. and Guney, K. (2006), "Phase inductance estimation for switched reluctance motor using adaptive neuro-fuzzy inference system", *Energy Convers. Manage.*, **47**(5), 485-493.

Dwaikat, M.B. and Kodur, V.K.R. (2009), "Hydrothermal model for predicting fire-induced spalling in concrete structural systems", *Fire Saf. J.*, **44**(3), 425-434. https://doi.org/10.1016/J.FIRESAF.2008.09.001.

Erdem, H. (2017), "Predicting residual moment capacity of thermally insulated RC beams exposed to fire using artificial neural networks", *Comput. Concrete*, **19**(6), 711. https://doi.org/10.12989/CAC.2017.19.6.711.

Eredm, R.T., Kantar, E., Gucuyen, E. and Anil, O. (2013), "Estimation of compression strength of polypropylene fibre reinforced concrete using artificial neural networks", *Comput. Concrete*, **12**(5), 613-625. https://doi.org/10.12989/cac.2013.12.5.613.

Hass, R. (1986), "Practical rules for the design of reinforced concrete and composite columns submitted to fire", Technical Report, Vol. 69, T.U. Braunschweig.(in German)

Hodhod, O.A., Said, T.E. and Ataya, A.M. (2018), "Prediction of creep in concrete using genetic programming hybridized with ANN", *Comput. Concrete*, **21**(5), 513. https://doi.org/10.12989/CAC.2018.21.5.513.

Ibrahimbegovic, A., Boulkertous, A., Davenne, L., Muhasilovic, M. and Pokrklic, A. (2010), "On modeling of fire resistance tests on concrete and reinforced-concrete structures", *Comput. Concrete*, **7**(4), 285-301. https://doi.org/10.12989/cac.2010.7.4.285.

Jang, J.S.R., Sun, C.T. and Mizutani, E. (1997), "Neuro-Fuzzy and Soft Computing-A Computational Approach to Learning and Machine Intelligence", *Automatic Control, IEEE*. https://doi.org/10.1109/TAC.1997.633847.

Kalifa, P., Chéné, G. and Gallé, C. (2001), "High-temperature behaviour of HPC with polypropylene fibres -From spalling to microstructure", *Cement Concrete Res.*, **31**(10), 1487-1499. https://doi.org/10.1016/S0008-8846(01)00596-8.

Khoury, G.A. (2000), "Effect of fire on concrete and concrete structures", *Pr. Struct. Eng. Mater.*, **2**(4), 429-447. https://doi.org/10.1002/pse.51.

Kisi, Ö. and Çobaner, M. (2009), "Modeling river stage-discharge relationships using different neural network computing techniques", *CLEAN -Soil, Air, Water*, **37**(2), 160-169. https://doi.org/10.1002/clen.200800010.

Klingsch, E.W.H. (2014), "Explosive spalling of concrete in fire", PhD Thesis, ETH Zürich, Zürich.

Kodur, V. and McGrath, R. (2003), "Fire endurance of highstrength concrete columns", *Fire Technol.*, **39**(1), 73-87. https://doi.org/10.1023/A:1021731327822.

Kodur, V.K.R. (2018), "Innovative strategies for enhancing fire performance of high-strength concrete structures", *Adv. Struct. Eng.*, **21**(11), 1723-1732. https://doi.org/10.1177/1369433218754335.

Kodur, V.K.R., Cheng, F., Wang, T., Latour, J. and Leroux, P. (2001), "Fire resistance of high-performance concrete columns", IRC-IR-834, National Research Council Canada.

Kodur, V.K.R., McGrath, R., Leroux, P. and Latour, J. (2005), "Experimental studies for evaluating the fire endurance of high-

strength concrete columns", Internal Report 81, National Research Council Canada.
Kodur, V.K.R., McGrath, R., Leroux, P., Latour, J. and MacLaurin, J. (2000), "Experimental studies on the fire endurance of high-strength concrete columns", National Research Council Canada.
Koza, J.R. (1992), "A genetic approach to finding a controller to back up a tractor-trailer truck", *Proceedings of the 1992 American Control Conference*, 2307-2311. https://doi.org/https://doi.org/10.23919/ACC.1992.4792548.
Lee, E.W.M., Yuen, R.K.K., Lo, S.M., Lam, K.C. and Yeoh, G.H. (2004), "A novel artificial neural network fire model for prediction of thermal interface location in single compartment fire", *Fire Saf. J.*, **39**(1), 67-87. https://doi.org/10.1016/S0379-7112(03)00092-4.
Lie, T. and Woollerton, J. (1988), *Fire Resistance of Reinforced Concrete Columns*, NRC Publications Archive, National Research Council Canada.
Lingam, A. and Karthikeyan, J. (2014), "Prediction of compressive strength for HPC mixes containing different blends using ANN", *Comput. Concrete*, **13**(5), 621-632. https://doi.org/10.12989/cac.2014.13.5.621.
Liu, J.C., Tan, K.H. and Yao, Y. (2018), "A new perspective on nature of fire-induced spalling in concrete", *Constr. Build. Mater.*, **184**(1), 581-590. https://doi.org/10.1016/j.conbuildmat.2018.06.204.
Mansouri, I. and Kisi, O. (2015), "Prediction of debonding strength for masonry elements retrofitted with FRP composites using neuro fuzzy and neural network approaches", *Compos. Part B: Eng.*, **70**, 247-255. https://doi.org/10.1016/J.COMPOSITESB.2014.11.023.
Mansouri, I., Gholampour, A., Kisi, O. and Ozbakkaloglu, T. (2018), "Evaluation of peak and residual conditions of actively confined concrete using neuro-fuzzy and neural computing techniques", *Neur. Comput. Appl.*, **29**(3), 873-888. https://doi.org/10.1007/s00521-016-2492-4.
Meacham, B., Engelhardt, M. and Kodur, V. (2009), "Collection of data on fire and collapse, faculty of architecture building", NSF *Engineering Research and Innovation Conference*, Honolulu, Hawaii. http://efectis.com/nl_en/index.htm.
Myllymaki, J. and Lie, T. (1991), *Fire Resistance Test of a Square Reinforced Concrete Column*, National Research Council Canada.
Naji, S., Shamshirband, S., Basser, H., Alengaram, U.J., Jumaat, M.Z. and Amirmojahedi, M. (2016), "Soft computing methodologies for estimation of energy consumption in buildings with different envelope parameters", *Energy Efficiency*, **9**(2), 435-453. https://doi.org/10.1007/s12053-015-9373-z.
Naser, M., Abu-Lebdeh, G. and Hawileh, R. (2012), "Analysis of RC T-beams strengthened with CFRP plates under fire loading using ANN", *Constr. Build. Mater.*, **37**, 301-309. https://doi.org/10.1016/j.conbuildmat.2012.07.001.
Naser, M.Z. (2011), "Behavior of RC beams strengthened with CFRP laminates under fire-A finite element simulation", American University of Sharjah. https://dspace.aus.edu/xmlui/handle/11073/2729.
Naser, M.Z. (2018), "Deriving temperature-dependent material models for structural steel through artificial intelligence", *Constr. Build. Mater.*, **191**, 56-68. https://doi.org/10.1016/J.CONBUILDMAT.2018.09.186.
Naser, M.Z. (2019), "Heuristic machine cognition to predict fire-induced spalling and fire resistance of concrete structures", *Auto. Constr.*, **106**, 102916. https://doi.org/10.1016/J.AUTCON.2019.102916.
Naser, M.Z. and Chehab, A. (2018), "Materials and design concepts for space-resilient structures", *Pr. Aerosp. Sci.*, **98**, 74-90. https://doi.org/10.1016/j.paerosci.2018.03.004.
Naser, M.Z. and Seitllari, A. (2019), "Concrete under fire: an assessment through intelligent pattern recognition", *Eng. Comput.*, 1-14. https://doi.org/10.1007/s00366-019-00805-1.
Peris-Sayol, G., Paya-Zaforteza, I., Balasch-Parisi, S. and Alós-Moya, J. (2017), "Detailed analysis of the causes of bridge fires and their associated damage levels", *J. Perform. Constr. Facil.*, **31**(3), 04016108. https://doi.org/10.1061/(ASCE)CF.1943-5509.0000977.
Phan, L.T. and Carino, N.J. (2000), "Fire performance of high strength concrete: Research needs", *Adv. Technol. Struct. Eng.*, ASCE, Reston, VA. https://doi.org/10.1061/40492(2000)181.
Rodrigues, J.P.C., Laím, L. and Correia, A.M. (2010), "Behaviour of fiber reinforced concrete columns in fire", *Compos. Struct.*, **92**, 1263-1268. https://doi.org/10.1016/j.compstruct.2009.10.029.
Saha, P., Prasad, M.L.V. and Kumar, P.R. (2017), "Predicting strength of SCC using artificial neural network and multivariable regression analysis", *Comput. Concrete*, **20**(1), 31. https://doi.org/10.12989/CAC.2017.20.1.031.
Seitllari, A. (2014), "Traffic flow simulation by Neuro-Fuzzy approach", *Second International Conference on Traffic*, Belgrade. https://trid.trb.org/view/1408239.
Seitllari, A. and Kutay, M.E. (2018), "Soft computing tools to predict progression of percent embedment of aggregates in chip seals", *Tran. Res. Record*, **2672**(12), 32-39.. https://doi.org/10.1177/0361198118756868.
Seitllari, A., Kumbargeri, Y., Bilgiri, K. and Boz, I. (2019), "A soft computing approach to predict and evaluate asphalt mixture aging characteristics using asphaltene as a performance indicator", *Mater. Struct.*, (pre-print).
Shah, A.H. and Sharma, U.K. (2017), "Fire resistance and spalling performance of confined concrete columns", *Constr. Build. Mater.*, **156**, 161-174. https://doi.org/10.1016/j.conbuildmat.2017.08.167.
Yavuz, G. (2019), "Determining the shear strength of FRP-RC beamsusing soft computing and code methods", *Comput. Concrete*, **23**(1), 49. https://doi.org/10.12989/CAC.2019.23.1.049.
Zadeh, L.A. (1995), "Discussion: Probability theory and fuzzy logic are complementary rather than competitive", *Technometrics*, **37**(3), 271-276. https://doi.org/10.1080/00401706.1995.10484330.
Zhang, B., Cullen, M. and Kilpatrick, T. (2016), "Spalling of heated high performance concrete due to thermal and hygric gradients", *Adv. Concrete Constr* **4**(1), 1-14. https://doi.org/10.12989/acc.2016.4.1.001.

CC

Appendix

Reference	Considered inputs				Observation	Applied modeling technique			
	fc (MPa)	*Brc* (mm)	*e* (mm)*	*P* (kN)		MLR	ANN	ANFIS	GA
(Rodrigues *et al.* 2010)	23.8	250	0	686	No spalling	No spalling	No spalling	No spalling	No spalling
	25.1	250	0	686	No spalling	No spalling	No spalling	No spalling	No spalling
	27	250	0	686	No spalling	No spalling	No spalling	No spalling	No spalling
	29.4	250	0	686	Spalling	No spalling	No spalling	No spalling	Spalling
(Buch and Sharma 2019)	27	300	20.03	544	Spalling	No spalling	Spalling	No spalling	Spalling
	28	300	0	544	Spalling	No spalling	Spalling	No spalling	Spalling
	28	300	20.03	532	Spalling	No spalling	Spalling	No spalling	Spalling
	31	300	39.84	567	Spalling	No spalling	Spalling	Spalling	Spalling
	31	300	39.84	567	Spalling	No spalling	Spalling	Spalling	Spalling
	32	300	20.03	579	Spalling	No spalling	Spalling	No spalling	Spalling
	58	300	20.03	892	Spalling	Spalling	Spalling	Spalling	Spalling
	60	300	39.84	892	Spalling	Spalling	Spalling	Spalling	Spalling
	67	300	20.03	996	Spalling	Spalling	Spalling	Spalling	Spalling
	69	300	0	1008	Spalling	Spalling	Spalling	Spalling	Spalling
	69	300	20.03	973	Spalling	Spalling	Spalling	Spalling	Spalling
(Shah and Sharma 2017)	34	300	0	1170	No spalling	No spalling	No spalling	No spalling	No spalling
	34	300	0	1170	No spalling	No spalling	Spalling	No spalling	No spalling
	34	300	0	1170	No spalling	No spalling	Spalling	No spalling	No spalling
	34	300	0	1170	No spalling	Spalling	Spalling	Spalling	No spalling
	34	300	0	1170	Spalling	No spalling	Spalling	No spalling	No spalling
	34	300	0	1170	Spalling	No spalling	Spalling	No spalling	No spalling
	63	300	0	1858	Spalling	Spalling	Spalling	Spalling	Spalling
	63	300	0	1858	Spalling	Spalling	Spalling	Spalling	Spalling
(Lie and Woollerton 1988)	34.2	305	0	0	No spalling	No spalling	No spalling	No spalling	No spalling
	34.8	305	0	1778	No spalling	No spalling	No spalling	No spalling	No spalling
	36.9	305	0	1333	No spalling	No spalling	No spalling	No spalling	No spalling
	37.6	305	0	1067	Spalling	Spalling	Spalling	Spalling	Spalling
	37.9	305	24.97	1178	No spalling	No spalling	No spalling	No spalling	No spalling
	38.3	305	0	1333	No spalling	No spalling	No spalling	No spalling	No spalling
	39.3	305	0	1000	No spalling	Spalling	Spalling	Spalling	No spalling
	39.9	305	0	1778	No spalling	No spalling	No spalling	No spalling	No spalling
	41.6	305	0	342	Spalling	No spalling	No spalling	No spalling	Spalling
	42.1	203	0	756	No spalling	No spalling	No spalling	No spalling	No spalling
	42.5	305	0	947	No spalling	No spalling	No spalling	No spalling	No spalling
	43.6	305	0	1044	No spalling	No spalling	No spalling	No spalling	No spalling
	46.6	305	0	1076	No spalling	No spalling	No spalling	No spalling	No spalling
	34.2	305	0	800	No spalling	No spalling	No spalling	No spalling	No spalling
	35.4	305	0	916	No spalling	No spalling	No spalling	No spalling	No spalling
	40.9	305	0	800	No spalling	No spalling	No spalling	No spalling	No spalling
	42.5	305	0	1413	No spalling	Spalling	Spalling	Spalling	No spalling
	35.1	305	0	711	No spalling	No spalling	No spalling	No spalling	No spalling
	36.9	305	0	1067	No spalling	No spalling	No spalling	No spalling	No spalling
	42.6	305	0	978	No spalling	No spalling	No spalling	No spalling	No spalling
	52.9	305	0	1178	No spalling	No spalling	No spalling	No spalling	No spalling
	37.1	305	0	1333	No spalling	Spalling	Spalling	Spalling	No spalling
	39.9	305	24.97	1000	No spalling	No spalling	No spalling	No spalling	No spalling
	40.7	406	0	0	No spalling	No spalling	No spalling	No spalling	No spalling
	49.5	305	0	1067	No spalling	No spalling	No spalling	No spalling	No spalling
	38.8	406	0	2418	No spalling	No spalling	No spalling	No spalling	No spalling
	42.3	203	0	169	No spalling	No spalling	No spalling	No spalling	No spalling
	36.1	305	0	1067	No spalling	No spalling	No spalling	No spalling	No spalling
	38.4	406	0	2795	No spalling	No spalling	No spalling	No spalling	No spalling
	39.6	305	0	800	No spalling	No spalling	No spalling	No spalling	No spalling
	46.2	406	0	2978	No spalling	No spalling	No spalling	No spalling	No spalling

Reference	Considered inputs				Observation	Applied modeling technique			
	fc (MPa)	*Brc* (mm)	*e* (mm)*	*P* (kN)		MLR	ANN	ANFIS	GA
(Myllymaki and Lie 1991)	37.8	300	0	1400	Spalling	No spalling	Spalling	No spalling	Spalling
(Kodur *et al*. 2000)	86	406	0	2406	Spalling	Spalling	Spalling	Spalling	Spalling
	89.6	406	0	2934	Spalling	Spalling	Spalling	Spalling	Spalling
	96	406	0	4919	Spalling	Spalling	Spalling	Spalling	Spalling
	119.7	305	0	2363	Spalling	Spalling	Spalling	Spalling	Spalling
	119.7	305	0	2954	Spalling	No spalling	No spalling	No spalling	Spalling
	119.7	305	24.97	2954	Spalling	No spalling	No spalling	No spalling	Spalling
	126.5	406	0	2913	Spalling	Spalling	Spalling	Spalling	Spalling
	99.7	406	0	3080	Spalling	Spalling	Spalling	Spalling	Spalling
(Kodur *et al*. 2001)	40.2	305	24.97	1000	No spalling	Spalling	Spalling	Spalling	No spalling
	40.2	305	0	1500	Spalling	Spalling	Spalling	Spalling	Spalling
	68.9	305	0	1800	No spalling	Spalling	Spalling	Spalling	No spalling
	68.9	305	0	2200	Spalling	Spalling	Spalling	Spalling	Spalling
	68.9	305	24.97	1500	Spalling	No spalling	Spalling	No spalling	Spalling
	73.4	305	0	1800	Spalling	Spalling	Spalling	Spalling	Spalling
	73.4	305	0	2200	Spalling	Spalling	Spalling	Spalling	Spalling
	73.4	305	24.97	1500	Spalling	Spalling	Spalling	Spalling	Spalling
	72.7	305	0	2000	No spalling	Spalling	Spalling	Spalling	No spalling
	72.7	305	0	1300	Spalling	Spalling	Spalling	Spalling	Spalling
	99.6	305	0	2000	Spalling	Spalling	Spalling	Spalling	Spalling
	99.6	305	0	2000	Spalling	Spalling	Spalling	Spalling	Spalling
	99.6	305	0	3000	Spalling	Spalling	Spalling	Spalling	Spalling
	119.7	305	0	1979	Spalling	Spalling	Spalling	Spalling	Spalling
(Kodur *et al*. 2005)	85	406	0	3895	No spalling	No spalling	No spalling	No spalling	No spalling
	85	406	0	4328	Spalling	Spalling	Spalling	Spalling	Spalling
	85	406	0	4328	Spalling	Spalling	Spalling	Spalling	Spalling
	114	406	0	4567	Spalling	No spalling	Spalling	No spalling	Spalling
	114	406	0	5373	Spalling	Spalling	Spalling	Spalling	Spalling
	114	406	0	3546	Spalling	No spalling	No spalling	No spalling	Spalling
	138	406	26.94	4233	Spalling	Spalling	Spalling	Spalling	Spalling
	138	406	26.94	4981	Spalling	Spalling	No spalling	No spalling	Spalling
	138	406	26.94	4981	Spalling	Spalling	Spalling	Spalling	Spalling
	40.2	305	0	930	No spalling	No spalling	No spalling	No spalling	No spalling
	138	406	26.94	4981	Spalling	Spalling	Spalling	Spalling	Spalling
	72.7	305	24.97	1200	Spalling	Spalling	Spalling	Spalling	Spalling

Note: the highlighted columns were randomly selected, statistically evaluated and included in testing dataset.
*The exponential of measured eccentricity value was used for developing MLR, ANN and ANFIS models.